

## Dynamic behaviors of the bridge considering pounding and friction effects under seismic excitations

Sang-Hyo Kim<sup>†</sup> and Sang-Woo Lee<sup>‡</sup>

*Department of Civil Engineering, Yonsei University, Seoul 120-749, Korea*

Ho-Seong Mha<sup>‡†</sup>

*Department of Civil Engineering, Hoseo University, Asan 336-795, Korea*

**Abstract.** Dynamic responses of a bridge system with several simple spans under longitudinal seismic excitations are examined. The bridge system is modeled as the multiple oscillators and each oscillator consists of four degrees-of-freedom system to implement the poundings between the adjacent oscillators and the friction at movable supports. Pounding effects are considered by introducing the impact elements and a bi-linear model is adopted for the friction force. From the parametric studies, the pounding is found to induce complicated seismic responses and to restrain significantly the relative displacements between the adjacent units. The smaller gap size also restricts more strictly the relative displacement. It is found that the relative displacements between the abutment and adjacent pier unit become much larger than the responses between the inner pier units. Consequently, the unseating failure could take a place between the abutment and nearby pier units. It is also found that the relative displacements of an abutment unit to the adjacent pier unit are governed by the pounding at the opposite side abutment.

**Key words:** bridge system; seismic excitation; pounding; friction; impact element; abutment; unseating failure.

---

### 1. Introduction

The bridge system with several simple spans can be described as the combination of multiple vibration units, and the global dynamic behaviors of such a bridge system become complicated due to interactions between the adjacent oscillating units. The interactions are produced mainly due to different dynamic characteristics of the oscillating units. In addition the out-of-phase characteristics between input seismic excitations due to the different traveling distances up to the different piers may disturb the responses to be out of phase even for the oscillating units with identical dynamic characteristics. There are various factors influencing bridge motions, such as inelastic behaviors of RC piers, foundation motions (rotation and translation) due to ground conditions, bridge-abutment-backfill interaction, pounding between adjacent girders, friction at movable supports, and so forth. The pounding phenomena of adjacent girders during earthquakes have been widely observed

---

<sup>†</sup> Professor

<sup>‡</sup> Graduate Student

<sup>‡†</sup> Assistant Professor

(Rosenblueth and Meli 1986, Kasai and Maison 1991). The phenomena are usually caused by different vibrating frequencies of individual units. Also, the induced relative motions between the adjacent vibration units produce the friction forces at movable supports while vibrating under seismic excitations. The pounding and friction may play important roles upon the global dynamic responses of the total bridge motions (Watanabe *et al.* 1998). The pounding may cause severe local damages to girder ends as well as bearings. Furthermore it may cause the superstructure unseating from movable supports, which is one of the major causes of bridge collapse (Malhotra *et al.* 1995, Priestley *et al.* 1996). Therefore, the analysis tool is desired to predict the dynamic behavior of the bridge system properly, which can unveil the effects of both pounding and friction.

In this study, the idealized mechanical model for the multi-simple span bridge system, which can consider both pounding and friction, is proposed. The pounding system with friction is modeled as a multi degree-of-freedom system, which is composed of individual mass-spring-damper systems connected to each other by the impact and friction elements. The bridge motions are evaluated by adopting the direct numerical integration technique using the derived equations of motion. The system only considering the friction at the movable supports is first analyzed to evaluate the main effects of the friction. The pounding system with friction is then examined to verify the effects on the characteristics of the response behaviors of the bridge system. Also considered is the influence from the various bridge-abutment-backfill interactions upon the inner bridge system motions.

## 2. Modeling of systems

### 2.1. Bridge model

The bridge considered is a three-span simple plate girder bridge with 35m span length as shown in Fig. 1. Piers of bent-type, shallow foundations, and seat-type abutments are used. The column height is 12m. In this study, only the longitudinal motions are in concern, so the total system can be divided into four individual vibrating units as shown in the Fig. 1.

To perform the analysis more efficiently, a simplified mechanical model is proposed using the lumped mass system, which is depicted in Fig. 2. In the figure,  $m_1, m_5, m_9$ =masses of superstructures,  $m_2, m_6$ =masses of piers,  $m_3, m_7$ =masses of foundations,  $m_4, m_8$ =rotational mass moments of inertia of foundations,  $m_{A1}, m_{A3}$ =masses of abutments, and  $m_{A2}, m_{A4}$ =rotational mass moments of inertia of abutments.  $K_2, K_6$  and  $C_2, C_6$  are the stiffness and damping constants of the piers,  $K_3, K_7$  and  $C_3, C_7$  are the translational stiffness and damping constants of the foundations, and  $K_4, K_8$  and  $C_4, C_8$  are

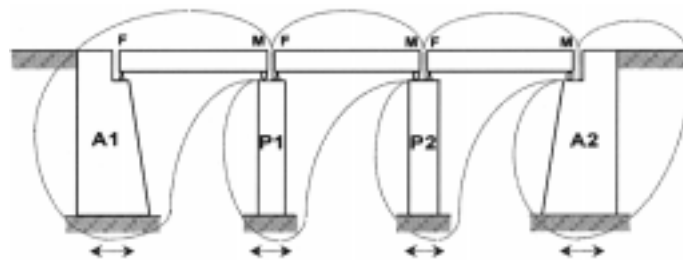


Fig. 1 Bridge model

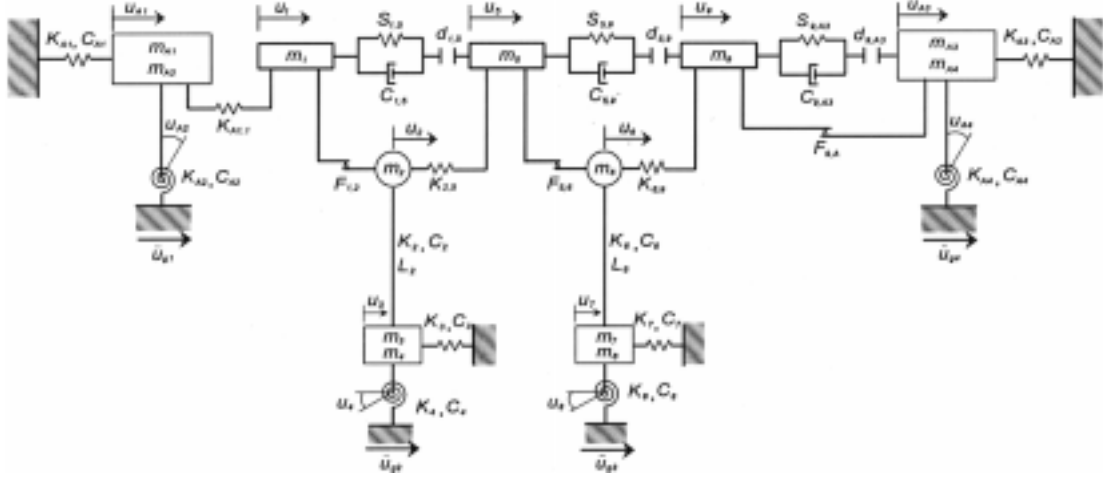


Fig. 2 Simplified mechanical model of the bridge

the rotational stiffness and damping constants of the foundations, respectively.  $K_{A1}, K_{A3}$  and  $C_{A1}, C_{A3}$  are the translational stiffness and damping constants of the abutments, and  $K_{A2}, K_{A4}$  and  $C_{A2}, C_{A4}$  are the rotational stiffness and damping constants of the abutments.  $K_{A1,1}, K_{2,5}$  and  $K_{6,9}$  are the stiffness of the fixed supports at individual vibration units.  $F_{1,2}, F_{5,6}$ , and  $F_{9,A}$  are the friction forces at the movable supports.  $S_{1,5}, S_{5,9}, S_{9,A3}$  and  $C_{1,5}, C_{5,9}, C_{9,A3}$  are the stiffness and damping constants of the impact elements. and  $L$  is height of pier.  $u_1, u_5, u_9$  are the displacements of the superstructures,  $u_2, u_6$  are the displacements at the top of piers,  $u_3, u_7$  are the translational displacements of the foundations,  $u_4, u_8$  are the rotational displacements of the foundations,  $u_{A1}, u_{A3}$ , are the translational displacements of the abutments,  $u_{A2}, u_{A4}$ , are the rotational displacements of the abutments, and  $\ddot{u}_g$  is the ground acceleration.

### 2.2. Pounding between girders

Two adjacent vibration units may produce pounding upon the applied seismic excitations with various intensities, and the pounding is governed by the relative displacements between two units. The pounding phenomenon can be described by a spring-damper element or by applying the impact law of mechanics for particles. It is known that the former approach can provide a better approximation to the real problem, under the condition that appropriate values for the properties of the spring-damper element are used (Anagnostopoulos 1995). The pounding is described in this study by placing spring-damper element (impact element) between the masses as shown in Fig. 3. The pounding condition is defined as follows.

$$\delta_i = u_i - u_{i+4} + u_{gi} - u_{g(i+1)} - d_{i,i+4} \geq 0 \quad (1)$$

where,  $u_i, u_{i+4}$  = the displacement of mass  $m_i$  and  $m_{i+4}$ ,  $u_{gi}, u_{g(i+1)}$  = the ground displacement, and  $d_{i,i+4}$  = the distance between  $m_i$  and  $m_{i+4}$ . Then the force due to pounding between  $m_i$  and  $m_{i+4}$  can be expressed as follows:

$$F_{i,i+4} = S_{i,i+4} \delta_i + C_{i,i+4} \dot{\delta}_i \quad \text{for } \delta_i > 0, \quad \text{otherwise } F_{i,i+4} = 0 \quad (2)$$

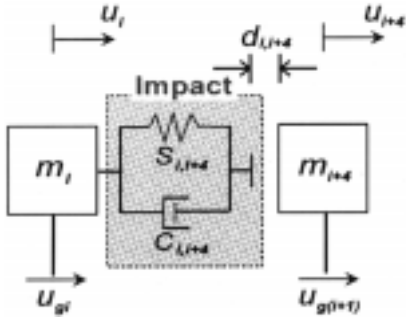


Fig. 3 Idealization of pounding between adjacent vibration units

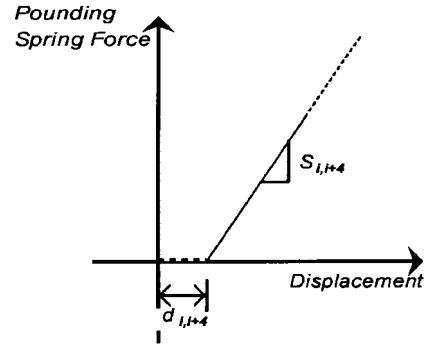


Fig. 4 Pounding spring force-displacement relationship

where  $S_{i,i+4}$  and  $C_{i,i+4}$  are the spring stiffness and damping constant of impact element, respectively. The pounding spring force-displacement relationship is shown in Fig. 4. The stiffness of spring is typically large and highly uncertain due to the unknown geometry of the impact surfaces, uncertain material properties under impact loadings, and variable impact velocities, etc. Based on a sensitivity study, it is known that the system responses are not quite sensitive to changes in the stiffness of spring (Anagnostopoulos 1988, Davis 1988, Maison and Kasai 1992). The damping constant which determines the amount of energy dissipated can be obtained by following relationship (Anagnostopoulos 1988).

$$C_{i,i+1} = 2\xi_i \sqrt{S_{i,i+1} \times m_i m_{i+1} / (m_i + m_{i+1})}, \quad \xi_i = -\ln r / \sqrt{\pi^2 + (\ln r)^2} \tag{3}$$

where,  $r$ =coefficient of restitution. Value of  $r=1$  ( $\xi=0$ ) describes fully elastic collision, while value of  $r=0$  ( $\xi=1$ ) represents perfectly plastic one.

### 2.3. Friction at the movable supports

The frictions between the superstructures and the movable supports is usually neglected in the bridge dynamic analysis. However, this may not yield the appropriate results since it ignores the energy dissipation due to the friction. In this study, a modified bilinear coulomb friction model is utilized. The simple model of the friction element between the superstructure and the support is described in Fig. 5. The relationship between the friction force and relative velocity between the adjacent oscillators can be depicted as shown in Fig. 6. In stick condition, the friction force increases up to a given value,  $\varepsilon$  of the relative velocity and then sustains a constant friction force multiplying vertical force with friction coefficient. The friction forces of the stick and sliding conditions,  $F_{i,i+1}$  are expressed as follows:

$$F_{i,i+1} = \begin{cases} \frac{1}{2} \mu m_i g \frac{1}{\varepsilon} \Delta_i & \text{for } |\Delta_i| < \varepsilon \\ \frac{1}{2} \mu m_i g & \text{for } |\Delta_i| \geq \varepsilon \end{cases} \tag{4}$$

where  $\mu$ =friction coefficient,  $\Delta_i = \dot{u}_i - \dot{u}_{i+1} + \dot{u}_{g(i)} - \dot{u}_{g(i+1)}$

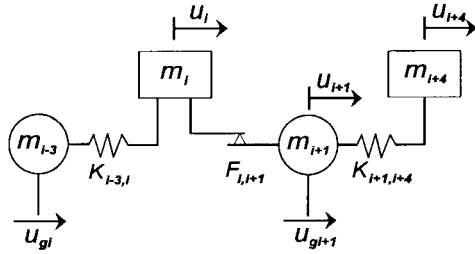


Fig. 5 Friction element

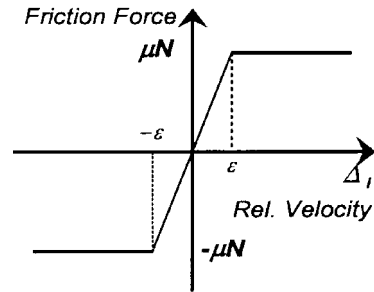


Fig. 6 Friction force-relative displacement relationship

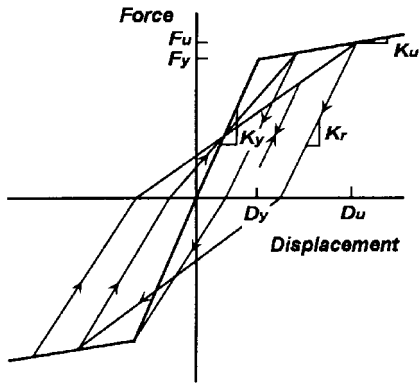


Fig. 7 Hysteretic model for RC pier

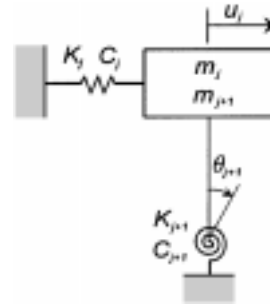


Fig. 8 Simplified model for the foundation and abutment

#### 2.4. Nonlinear piers, foundations, and abutment motions

The material nonlinearity of the RC pier can be described by adopting the hysteresis model obtained analytically from the moment-curvature curve based on the constitutive laws of the basic materials of piers. The restoring force characteristics of the pier is modeled as degrading-bilinear response as shown in Fig. 7. In Fig. 7,  $F_y$ ,  $F_u$ =yielding force and ultimate force of pier,  $D_y$ ,  $D_u$ =yielding displacement and ultimate displacement of pier, and  $K_y$ ,  $K_u$ ,  $K_r$ =elastic stiffness, strain-hardening stiffness, and unloading stiffness of pier, respectively. The geometric nonlinearity of RC pier is considered by using the  $P-\Delta$  effects.

Foundation and abutment are modeled with translational and rotational springs and dampers in order to consider ground conditions. The stiffness of foundation and abutment are determined according to Korean Standard Specification for Highway Bridges: Seismic Design. Fig. 8 is the simplified model of the foundation and abutment.

### 3. Equations of motion and seismic excitations

The governing equations of the motion of the system shown in Fig. 2 can be derived as follows:

$$m_{A1}\ddot{u}_{A1}+K_{A1}u_{A1}+C_{A1}\dot{u}_{A1}+K_{A1,1}(u_{A1}+u_{A2}\cdot H-u_1)=-m_{A1}\ddot{u}_{g1} \quad (5)$$

$$m_{A2}\ddot{u}_{A2}+K_{A2}u_{A2}+C_{A2}\dot{u}_{A2}+K_{A1,1}(u_{A1}+u_{A2}\cdot H-u_1)-K_{A1}\cdot H\cdot u_{A1}-C_{A1}\cdot H\cdot \dot{u}_{A1}=0 \quad (6)$$

$$m_1\ddot{u}_1-K_{A1,1}(u_{A1}+u_{A2}\cdot H-u_1)+F_{1,5}=-m_1\ddot{u}_{g1}+F_{1,2} \quad (7)$$

$$m_2\ddot{u}_2+K_{2,5}(u_5-u_2)+R_2-\frac{(m_2+m_5)g}{L_2}(u_2-u_3-L_2u_4)+C_2(\dot{u}_2-\dot{u}_3-L_2\dot{u}_4)=-m_2\ddot{u}_{g2}-F_{1,2} \quad (8)$$

$$m_3\ddot{u}_3-R_2+\frac{(m_2+m_5)g}{L_2}(u_2-u_3-L_2u_4)+K_3u_3-C_2(\dot{u}_2-\dot{u}_3-L_2\dot{u}_4)+C_3\dot{u}_3=-m_3\ddot{u}_{g2} \quad (9)$$

$$m_4\ddot{u}_4-L_2R_2+(m_2+m_5)g(u_2-u_3-L_2u_4)+K_4u_4-L_2C_2(\dot{u}_2-\dot{u}_3-L_2\dot{u}_4)+C_4\dot{u}_4=0 \quad (10)$$

$$m_5\ddot{u}_5+K_{2,5}(u_5-u_2)-F_{1,5}+F_{5,9}=-m_5\ddot{u}_{g2}+F_{5,6} \quad (11)$$

$$m_6\ddot{u}_6+K_{6,9}(u_9-u_6)+R_6-\frac{(m_6+m_9)g}{L_6}(u_6-u_7-L_6u_8)+C_6(\dot{u}_6-\dot{u}_7-L_6\dot{u}_8)=-m_6\ddot{u}_{g3}-F_{5,6} \quad (12)$$

$$m_7\ddot{u}_7-R_6+\frac{(m_6+m_9)g}{L_6}(u_6-u_7-L_6u_8)+K_7u_7-C_6(\dot{u}_6-\dot{u}_7-L_6\dot{u}_8)+C_7\dot{u}_7=-m_7\ddot{u}_{g3} \quad (13)$$

$$m_8\ddot{u}_8-L_6R_6+(m_6+m_9)g(u_6-u_7-L_6u_8)+K_8u_8-L_6C_6(\dot{u}_6-\dot{u}_7-L_6\dot{u}_8)+C_8\dot{u}_8=0 \quad (14)$$

$$m_9\ddot{u}_9+K_{6,9}(u_9-u_6)-F_{5,9}+F_{9,A3}=-m_9\ddot{u}_{g3}+F_{9,A} \quad (15)$$

$$m_{A3}\ddot{u}_{A3}+K_{A3}u_{A3}+C_{A3}\dot{u}_{A3}-F_{9,A3}=-m_9\ddot{u}_{g3}-F_{9,A} \quad (16)$$

$$m_{A4}\ddot{u}_{A4}+K_{A4}u_{A4}+C_{A4}\dot{u}_{A4}-K_{A3}\cdot H\cdot u_{A3}-C_{A3}\cdot H\cdot \dot{u}_{A3}=0 \quad (17)$$

where  $R_i$ 's are the restoring forces of piers obtained from hysteresis model for displacement presented as  $u_{i+1}-u_{i+2}-L_{i+1}u_{i+3}$ ,  $\ddot{u}_{g1}$ ,  $\ddot{u}_{g2}$ ,  $\ddot{u}_{g3}$ ,  $\ddot{u}_{g4}$  are the ground accelerations at the individual vibration units.  $H$  is the height of abutment.

For input excitations, the actual measured earthquakes may be the best for the analysis, but due to the lack of the real data, artificial seismic excitations are widely used in many cases. Input seismic excitations are produced by using the well known SIMQKE (Gasparini and Vanmarcke 1976),

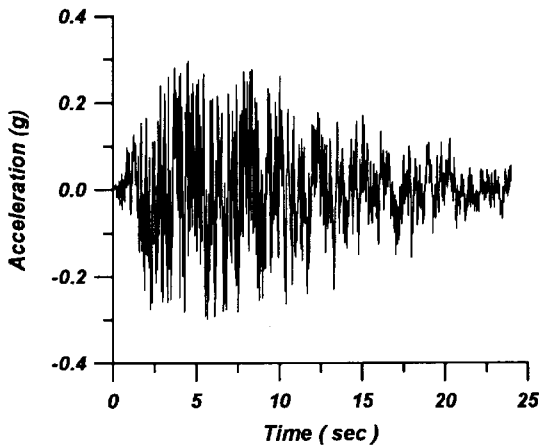


Fig. 9 Simulated seismic excitation

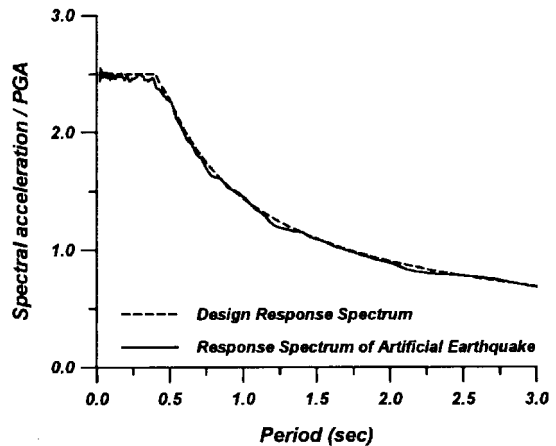


Fig. 10 Response spectrum

which are forced to be compatible to the design response spectra defined in the Korean Standard Specifications for Highway Bridges (1996).

An example of the simulated seismic excitation is shown in Fig. 9, and the comparison of the response spectrum and the given design response spectrum for damping ratio 5% is shown in Fig. 10. The result shows that the seismic excitations well matches the given design response spectrum.

#### 4. Results and observations

The dynamic analyses are conducted upon four different types of systems according to the consideration of the friction and pounding phenomena. Applied seismic excitations are generated with various PGA's from 0.1 g to 0.6 g. The seismic wave is assumed to have a propagating velocity of 760 m/sec and travel in the longitudinal direction, i.e., from one abutment to another. The 5cm-gap distance between adjacent vibration units is selected, and the friction coefficient at movable supports is assumed to be 0.05 based on the current practice. In the analysis, relative displacements between the adjacent vibration units of the bridge system are mainly examined to verify the effects of the pounding and friction phenomena upon the responses.

The mean values and 90% extreme values based on the Gumbel's Type-I distribution, of the maximum relative displacements (MRD) of all four different systems are prepared to verify the effects of pounding and friction upon the bridge motions. The results are tabulated in Table 1. The MRD's normalized by the responses obtained from the system without both pounding and friction are depicted in Fig. 11. The individual effects of either pounding or friction as well as the combined effect are well distinguished from Table 1 and Fig. 11. Especially between the abutment and pier vibration units, where the relative displacement is quite large due to the different vibration characters of two adjacent units compared with those between the pier and pier units, the effects show clear trends. Between abutment and nearby pier units (A1-P1 and P2-A2), the major effects of both pounding and friction are found to reduce the magnitudes of the relative motions. The friction tends to reduce more dramatically the relative motions than the pounding phenomenon under weak seismic excitations ( $PGA \leq 0.2$  g). For the moderate seismic excitations ( $PGA=0.3$  g), the reduced amounts of the MRD's due to pounding and friction are almost identical. For the stronger seismic excitations ( $PGA \geq 0.4$  g), the pounding reduces the relative displacements more dramatically than the friction, indicating that it dominates the relative motions under strong earthquakes. The pounding effects are found to be significant as the seismic loading becomes strong and reduce the relative displacement by up to 60% for the 90%-extreme values and 50% for the means under a strong excitation such as the case with PGA of 0.6 g. Since the pounding effects restrain the intensity as well as variation of the relative displacement, the 90% extreme values are diminished much more for higher PGA than the means.

The relative displacements between pier units (P1-P2) show the different trends. The frictions still reduces the relative motions while the pounding increases them. The relative motions between pier units without pounding are expected to be very small since the dynamic responses are almost the same to each other.

The figures in Fig. 12 contain the MRD's simulated and plotted on the Gumbel Type-I extreme distribution papers, in which the friction is considered for all cases. In the figures  $s=-\ln(-\ln p)$  and  $p=i/(N+1)$ .  $N$  is the number of simulations. The figures show the good fitness of the Gumbel Type-I as well as the reduced variance for the MRD's between the abutment and pier units.

Table 1 Simulated results of MRD's (unit: cm)

Friction Pounding	PGA	Without Friction			With Friction		
		A1-P1	P1-P2	P2-A2	A1-P1	P1-P2	P2-A2
Without Pounding	0.1g	5.97 (6.98)*	1.14 (1.31)	6.03 (6.44)	2.53 (3.52)	0.62 (0.72)	2.05 (2.92)
	0.2g	10.73 (13.72)	2.03 (2.33)	10.66 (13.18)	7.13 (8.98)	1.25 (1.53)	6.09 (7.87)
	0.3g	15.95 (20.43)	2.54 (3.23)	13.15 (17.27)	12.37 (15.72)	1.87 (2.38)	9.79 (13.08)
	0.4g	23.32 (33.70)	2.91 (3.65)	14.98 (25.01)	18.64 (24.75)	2.37 (3.49)	11.76 (17.59)
	0.5g	29.75 (45.74)	3.36 (4.22)	18.86 (33.49)	25.75 (38.68)	2.71 (4.18)	15.62 (25.71)
	0.6g	34.22 (50.73)	4.06 (4.75)	24.90 (40.26)	31.96 (50.29)	3.28 (5.01)	19.73 (33.45)
With Pounding	0.1g	5.76 (7.11)	2.08 (3.67)	5.82 (6.55)	2.53 (3.52)	0.62 (0.76)	2.05 (2.92)
	0.2g	8.43 (9.67)	6.51 (8.99)	8.25 (9.84)	7.53 (9.01)	1.03 (1.51)	6.33 (7.65)
	0.3g	12.01 (15.34)	7.24 (10.40)	9.91 (11.55)	10.39 (12.28)	4.03 (7.15)	8.60 (11.10)
	0.4g	13.23 (15.37)	8.46 (11.49)	10.95 (13.78)	13.53 (15.79)	3.52 (5.82)	10.75 (13.05)
	0.5g	14.58 (17.70)	8.49 (12.03)	12.28 (14.76)	15.14 (17.80)	5.68 (7.70)	11.40 (14.14)
	0.6g	17.16 (20.80)	9.98 (15.20)	13.90 (16.33)	16.79 (21.41)	5.08 (8.06)	13.36 (16.93)

\*( ): Gumbel Type-I 90% extreme values

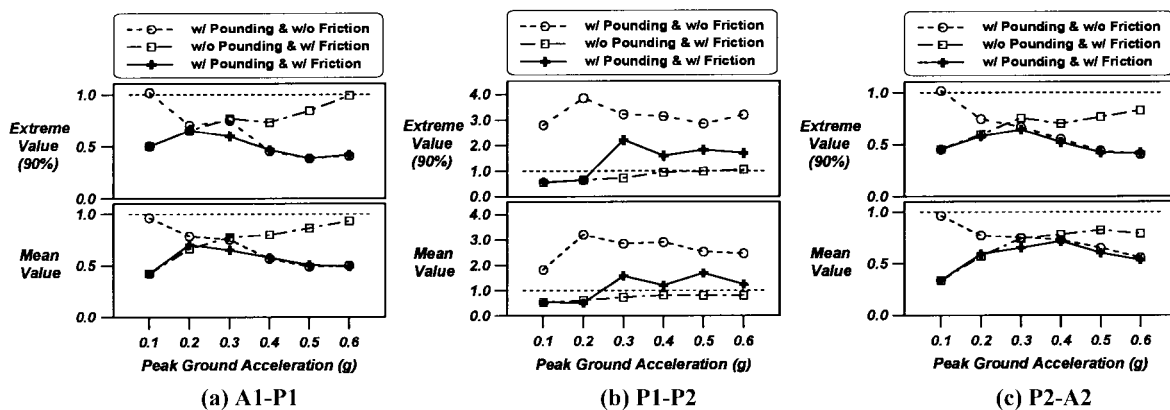


Fig. 11 Normalized results of MRD's

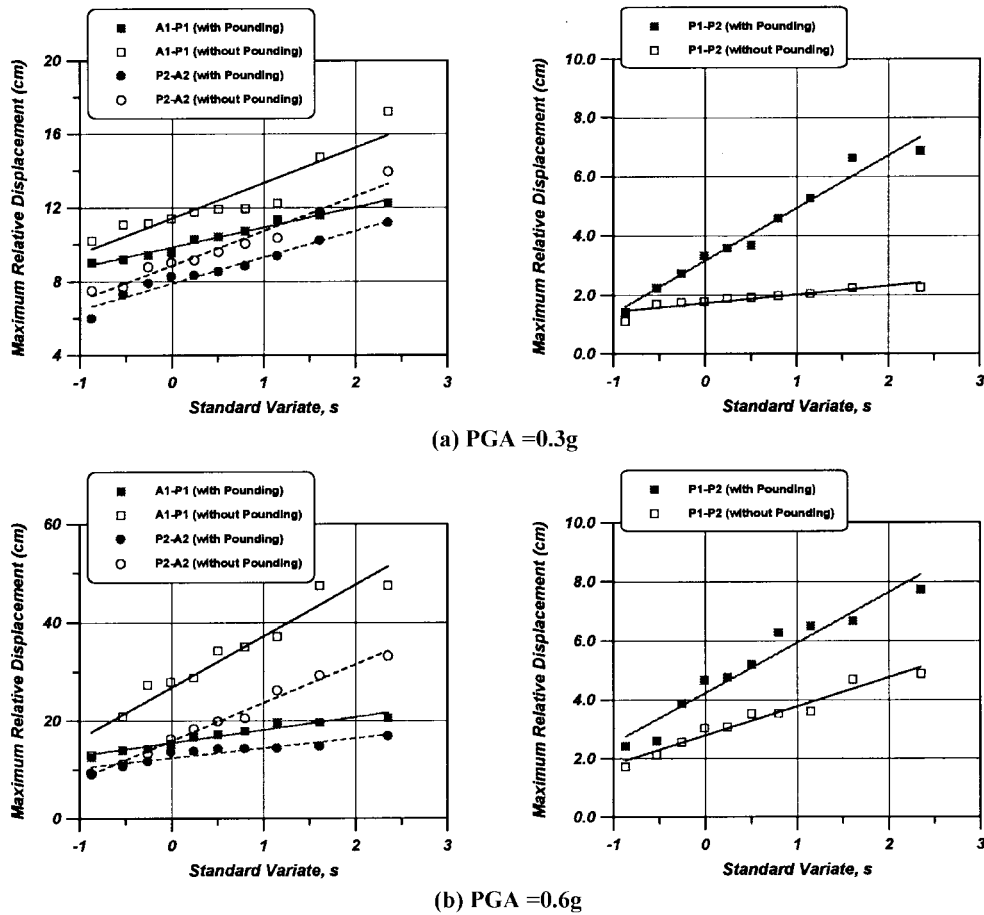


Fig. 12 MRD's plotted on the Gumbel Type-I probability paper (gap size=5 cm)

The relative behavior between the P1-P2 units is found to be influenced very considerably by the pounding with the adjacent abutment units and results in very large amplifications on the relative displacements. In addition, the MRD's show much large scattering and variance. However, the possibility of the undesired behavior, such as unseating failure of the superstructure, is still low since the absolute value of the relative displacement is very small because of the identical dynamic characteristics in the two vibration units.

The Fig. 13 shows the typical examples of time histories showing the restraining effect of pounding on the relative displacement between the abutment and pier units as well as the interruption (or hammering effect) on the behavior of the pier units. The figures in Fig. 14 demonstrate the combined effects of the pounding and friction more clearly.

Next, the effect of the gap size upon the responses is examined by investigating the MRD's for the systems with two different gap sizes of 5 cm and 10 cm. The simulated results are summarized in Table 2 for two different levels of PGA's, 0.3 g and 0.6 g. As can be expected the smaller gap size restrains the relative displacements of the abutment units from the adjacent pier vibration units more tightly, especially under strong excitations such as the case of PGA=0.6 g, due to more frequent pounding phenomena. However, the MRD's between P1-P2 become less for the case with

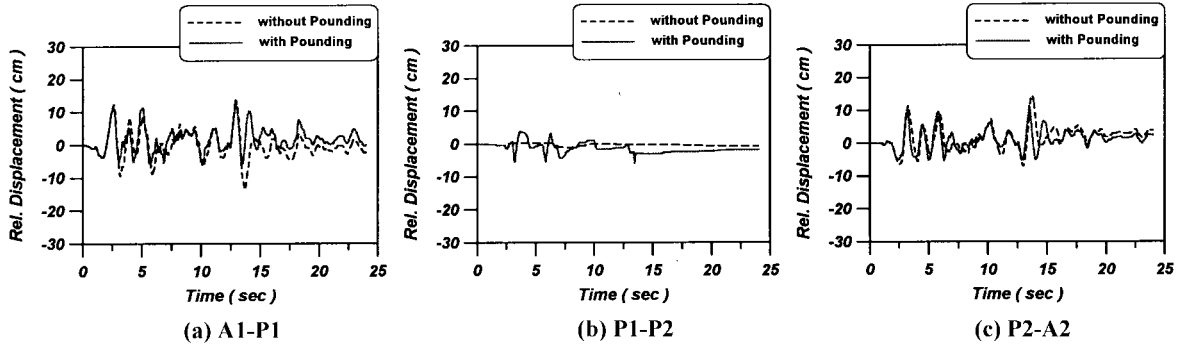


Fig. 13 Time histories of relative displacements between adjacent vibration units (with friction, 0.3 g)

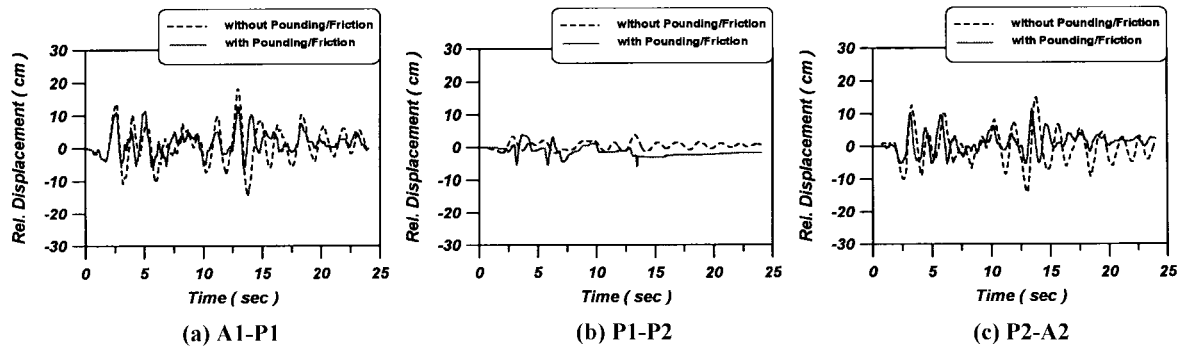


Fig. 14 Time histories of relative displacements between adjacent vibration units (0.3 g)

the wider gap size of 10 cm under moderate excitations of  $PGA=0.3$  g, since the pounding between the abutment and pier units does not occur often and thus the amplification on the responses of pier units are not triggered by pounding.

Finally, the dynamic behaviors of different bridge systems with 6 and 9 spans are investigated to examine the propagating effect of the abutment interaction upon the global bridge motions with various PGAs. The mean values and 90% extreme values of MRD's between abutment and pier units located at both left and right ends of the bridge systems are evaluated and tabulated in the Tables 3 and 4. For the bridge with small number of spans (3-span), the relative displacements

Table 2 MRD's according to gap size between vibration units (unit: cm)

Gap	0.3g			0.6g		
	A1-P1	P1-P2	P2-A2	A1-P1	P1-P2	P2-A2
5 cm	10.39 (12.28)*	4.03 (7.15)	8.60 (11.10)	15.14 (17.80)	5.68 (7.70)	11.40 (14.14)
10 cm	12.92 (16.52)	1.65 (2.21)	10.20 (13.21)	26.52 (32.66)	6.54 (12.68)	19.73 (25.50)

\*( ): Gumbel Type-I 90% extreme values

Table 3. Simulated results of MRD's between the left abutment and nearby pier units (unit: cm)

PGA	No friction & pounding	3-span (A1-P1)	6-span (A1-P1)	9-span (A1-P1)
0.1g	5.97 (6.98)*	2.53 (3.52)	4.36 (5.59)	4.65 (6.17)
0.2g	10.73 (13.72)	7.53 (9.01)	8.76 (11.21)	8.37 (11.10)
0.3g	15.95 (20.43)	10.39 (12.28)	12.54 (16.85)	11.88 (15.70)
0.4g	23.32 (33.70)	13.53 (15.79)	17.36 (24.62)	19.06 (27.60)
0.5g	29.75 (45.74)	15.14 (17.80)	28.35 (37.98)	28.09 (40.53)
0.6g	34.22 (50.73)	16.79 (21.41)	34.71 (44.94)	38.03 (51.43)

\*( ): Gumbel Type-I 90% extreme values

Table 4. Simulated results of MRD's between the right abutment and nearby pier units (unit: cm)

PGA	No friction & pounding	3-span (P2-A2)	6-span (P5-A2)	9-span (P8-A2)
0.1g	6.03 (6.44)*	2.05 (2.92)	2.90 (3.90)	2.92 (3.57)
0.2g	10.66 (13.18)	6.33 (7.65)	7.24 (8.62)	7.42 (8.93)
0.3g	13.15 (17.27)	8.60 (11.10)	11.10 (15.78)	11.11 (15.25)
0.4g	14.98 (25.01)	10.75 (13.05)	14.99 (19.87)	16.05 (21.29)
0.5g	18.86 (33.49)	11.40 (14.14)	20.38 (28.15)	21.98 (28.53)
0.6g	24.90 (40.26)	13.36 (16.93)	24.23 (33.84)	23.83 (30.90)

\*( ): Gumbel Type-I 90% extreme values

between the abutment units and their adjacent pier units are constrained by the motion of abutment in the opposite side, respectively. As the number of span increases, therefore, the constraining effect from the opposite abutment becomes diminished, producing the relatively larger responses. With the large number of spans (9-span), the mean and extreme values are found to converge to those of the bridge system without consideration of pounding and friction.

From the results, the pounding phenomena between the abutment and the nearby pier units are found to dominate the global motion, and the effect is propagated into the next pier units. The relative displacements between pier units are very small compared to those between the abutment and pier units, indicating that the relative motion near the abutment controls the span collapses. Therefore, the possibility of unseating failure of the superstructure spanning between the abutment

and pier may be much higher than the case of the pier to pier as far as the geometric conditions, such as span length, pier height, etc., are similar for the whole bridge system.

## 5. Conclusions

The dynamic behaviors of a multi-simple span bridge system under seismic excitations are examined with various conditions. An idealized analytical model is proposed, considering the pounding between the adjacent vibration units and the friction at the movable supports. The developed model is found to provide the appropriate information on the complicated seismic responses of the multi-simple span bridge.

Based on the results, the followings are drawn as conclusions:

- 1) The pounding effects are found to cause remarkable changes in the seismic responses and to reduce the relative displacements between the adjacent vibration units significantly under strong seismic excitations. Especially the pounding between the abutment and adjacent pier units is found to dominate and restrain the global bridge motion.
- 2) The effect of the friction is found to mainly reduce the seismic responses especially under weak seismic excitations ( $PGA \leq 0.2$  g).
- 3) Under weak seismic excitations ( $PGA \leq 0.2$  g), friction dominates the responses while the pounding starts to dominate the responses under stronger seismic excitations ( $PGA \geq 0.4$  g).
- 4) The smaller gap size between adjacent units restrains the relative displacements more tightly due to more frequent pounding phenomena.
- 5) It is found that the abutment in the opposite side constrains the relative motions inside abutments due to pounding, and that the constraining effect is diminished as the number of span increases.

From results, the relative displacements between the abutment units and their adjacent pier units become much larger than those between the pier units in the multi-simple span bridge with similar geometric conditions. Therefore, the possibility of the unseating failure of superstructures between the abutment and pier could be much higher than the case of the pier to pier.

## Acknowledgements

This work was supported by the Brain Korea 21 Project and the Korea Science and Engineering Foundation (KOSEF) through the KEERC.

## References

- Anagnopoulos, S.A. (1988), "Pounding of buildings in series during earthquakes", *Earthquake Engineering and Structural Dynamics*, **16**, 443-456.
- Anagnopoulos, S.A. (1995), "Earthquake induced pounding; State of the Art", *Tenth European Conference on Earthquake Engineering*, 897-905.
- Davis, R.O. (1988), "Pounding of buildings modeled by an impact oscillator", *Earthquake Engineering and Structural Dynamics*, **16**, 443-456.
- Gasparini, D.A. and Vanmarcke, E.H. (1976), "Evaluation of seismic safety of buildings simulated earthquake

- motions compatible with prescribed response spectra”, Massachusetts Ins. of Technology, Report 2.
- Kasai, K. and Maison, B.F. (1991), “Structural pounding”, *Reflections on the Loma Prieta Earthquake of October 17 1989*, Structural Engineers Association of California (SEAOC).
- Maison, B.F. and Kasai, K. (1992), “Dynamics of pounding when two buildings collide”, *Earthquake Engineering and Structural Dynamics*, **21**, 771-786.
- Malhotra, P.K., Huang, M.J. and Shakal, A.F. (1995), “Seismic interaction at separation joints of an instrumented concrete bridge”, *Earthquake Engineering Structural Dynamics*, **24**, pp.1055-1067.
- Ministry of Construction and Transportation (1996), “*Korean standard specifications for highway bridge*”.
- Priestley, M.J.N., Seible, F. and Calvi, G.M. (1996), “*Seismic design and retrofit of bridges*”, Wiley, New York.
- Rosenblueth, E. and Meli, R. (1986), “The 1985 Earthquake; Causes and effects in Mexico City”, *Concrete Ins.*, **8**(5).
- Watanabe, E., Kajita, Y., Sugiura, K., Nagata, K. and Maruyama, T. (1998), “Pounding of adjacent superstructures of elevated bridges under severe earthquake”, *Developments in Short and Medium Span Bridge Engineering*, 98.